COMPDYN 2011
ECCOMAS Thematic Conference on
Computational Methods in Structural Dynamics and Earthquake Engineering
M. Papadrakakis, M. Fragiadakis, V. Plevris (eds.)
Corfu, Greece, 25-28 May 2011

A MESHLESS METHOD FOR FLUID-STRUCTURE INTERACTIONS: APPLICATION TO THE FAILURE PREDICTION OF A TANK UNDER IMPACT

Fabien Caleyron[1,2], **Alain Combescure**[1], **Vincent Fauher**[2] **and Serguei Potapov**[2]

[1]Université de Lyon, CNRS, INSA-Lyon, LaMCoS UMR 5259
e-mail: {fabien.caleyron, alain.combescure}@insa-lyon.fr,

[2] LaMSID UMR EDF-CNRS-CEA 2832
e-mail: vincent.faucher@cea.fr, serguei.potapov@edf.fr

Keywords: meshless, SPH, shell, fluid, impact, failure.

Abstract. *The development of numerical methods for the simulation of thin structures in interaction with a fluid is an industrial issue. In particular, such simulations should be able to predict a possible failure of the shell and the resulting leakage rate in situations involving impacts. This kind of simulations involves three key components: a thin structural model that includes highly nonlinear behaviors leading to failure, a fluid model able to handle sloshing and spatters phenomena, and finally, fluid-structure interactions whose topology can change drastically during calculations. This paper presents a solution based on a meshless method called Smoothed Particles Hydrodynamics (SPH) which is used to model both the fluid and the shell. The fluid-structure interaction is handled via a unilateral contact algorithm adapted to the SPH context. The capabilities of the method are illustrated on several problems involving fracturing shells and by simulating an experiment involving fluid leakage of a tank impacted by a bullet.*

1 INTRODUCTION

The purpose of meshless methods is to discretize a domain with a set of nodes rather than elements for which the connectivity is fixed. The neighbourhood of each node can vary during the calculation which simplifies the treatment of large deformations, cracks and fractures. Meshless methods can be distinguished depending on the approximation functions they use as well as the formulation they rely on (strong or weak form). A detailed overview of meshless methods is presented in [1]. Methods based on the weak form of the equilibrium equations are generally more accurate and stable but the need to perform numerical integrations complicates the treatment of fractures. As a consequence, methods based on the strong form of the equilibrium equations are sometimes preferred to perform simulations involving impacts and fragmentations.

A full SPH fluid-shell interaction model is described in this paper. The SPH method relies on the strong form of the equilibrium equations and was one of the first proposed meshless method [2]. It is traditionally used in fluid dynamics, especially for the simulation of free surface flows. The method has recently been extended to structural dynamics and more specifically to shells theory [3]. This paper is the extension of [3] to the modeling of damage, fracture and failure.

The fundamentals of the SPH method and the corresponding fluid model are presented in the first section of the paper. Then, we explain the application of the SPH method to the Mindlin-Reissner's thick shells theory and its extension to fracture modeling in the second section. The Pinballs method [4] which is used to handle fluid-structure interactions is described in the third section. Finally, the simulation of a water filled tank impacted by a projectile is presented.

2 SPH METHOD AND SPH FLUID MODEL

2.1 SPH method

The SPH method discretizes the domain of interest Ω with a set of N nodes whose neighbourhood can vary in time. Each node represents a material amount m_i chosen so that the total mass of the structure is described correctly $m = \sum m_i$. Nodes interact one with each other through the use of functions for the approximation of a physical field or the approximation of its gradient. These functions have a compact support which means they are non-zero within a domain Ω_{V_i} (i.e. Ω_{V_i} is the neighbourhood of node i) and null elsewhere. The size of the neighbourhood Ω_{V_i} is a fundamental parameter of the method and is often denoted $2h$ in the SPH method. The B3 spline function is often used in the SPH method:

$$w_i(\overrightarrow{x_j}) = w_{ij} = C \begin{cases} \frac{3}{2}\left[\frac{2}{3} - \left(\frac{r_{ij}}{h}\right)^2 + \frac{1}{2}\left(\frac{r_{ij}}{h}\right)^3\right] \text{ if } 0 \leq \frac{r_{ij}}{h} \leq 1 \\ \frac{1}{4}\left[2 - \frac{r_{ij}}{h}\right]^3 \text{ if } 1 < \frac{r_{ij}}{h} < 2 \\ 0 \text{ otherwise} \end{cases} \tag{1}$$

where $r_{ij} = \|\overrightarrow{x_i} - \overrightarrow{x_j}\|$ and $C = 10/7\pi h^2$ in dimension 2. It is a normalization factor that is chosen to ensure the partition of unity property. The approximation of a field $\{f_j\}$, $j = \{1, ..., N\}$ and its gradient can be written:

$$f(\overrightarrow{x_i}) \approx \sum_{j \in \Omega_{V_i}} f_j w_{ij} V_j \tag{2}$$

$$\overrightarrow{\nabla} f(\overrightarrow{x_i}) \approx \sum_{j \in \Omega_{V_i}} f_j \overrightarrow{\nabla} w_{ij} V_j \tag{3}$$

where V_j is the material volume represented by node j.

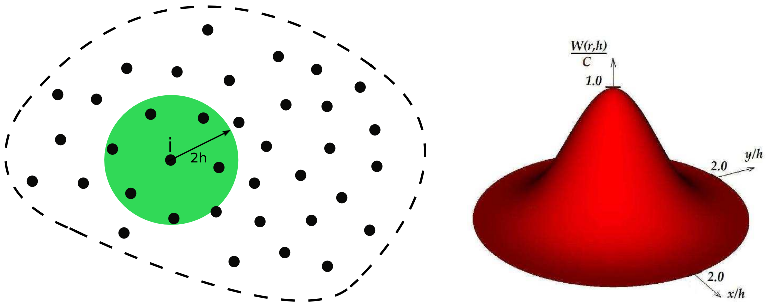

(a) Neighbourhood of an SPH node (b) Spline B3

Figure 1: Definition of the neighbourhood Ω_{V_i} through the B3 spline.

2.2 SPH fluid model

The fluid is assumed to be perfect, weakly compressible and acoustic. The governing equations, once discretized in the updated Lagrangian framework, can be written:

- equilibrium equation:

$$\left(\frac{\partial \overrightarrow{v}}{\partial t}\right)_i = - \sum_{j \in \Omega_{V_i}} m_j \left(\frac{p_i}{{\rho_i}^2} + \frac{p_j}{{\rho_j}^2}\right) \overrightarrow{\nabla} w_{ij} \tag{4}$$

  where p is the pressure, ρ density and $\overrightarrow{v}$ the velocity vector. We can notice that equation (4) is symmetric so it respects Newton's third law of motion.

- continuity equation:

$$\left(\frac{\partial \rho}{\partial t}\right)_i = \rho_i \sum_{j \in \Omega_{V_i}} \frac{m_j}{\rho_j} \left(\overrightarrow{v_i} - \overrightarrow{v_j}\right) \overrightarrow{\nabla} w_{ij} \tag{5}$$

  This equation was chosen because it cancels the density variations when the fluid flow is uniform.

- equation of state:

$$\Delta p_i = c^2 \Delta \rho_i \tag{6}$$

  where c is the speed of sound in the fluid.

Artificial linear and quadratic viscosity terms are used to stabilize calculations in presence of shocks.

3 FRACTURING SPH SHELL MODEL

This section presents the application of the SPH method to structural dynamics and more specifically to Mindlin-Reissner's thick shells theory. The model described in [3] is extended in this article for the modeling of shells damage and fracture.

3.1 SPH shell formulation (SPHS)

The SPH method presents three major drawbacks when it is applied to structural dynamics. They are well known and widely discussed in the literature where solutions are found:

- the method has bad consistency properties, especially near the boundary of the SPH domain where nodes have incomplete neighbourhoods. This drawback prevents the method from having good mesh convergence properties. The solution proposed in [5] consists in using Moving Least Square (MLS) approximation functions. These functions are constructed from a polynomial basis of degree n and, as a consequence, exhibit a n order consistency. The approximation in $\overrightarrow{x}$, built around $\overrightarrow{x}^*$, of a data field $\{u_i\}$, $i = \{1, ..., N\}$, is:
$$u(\overrightarrow{x}, \overrightarrow{x}^*) = \overrightarrow{p}^T(\overrightarrow{x})\overrightarrow{a}(\overrightarrow{x}^*) \tag{7}$$
$\overrightarrow{p}$ is the polynomial basis and $\overrightarrow{a}$ is a vector of coefficients obtained by minimizing the following weighted L_2 norm:
$$J = \sum_{j=1}^{N} \left[\overrightarrow{p}^T(\overrightarrow{x_j})\overrightarrow{a}(\overrightarrow{x}^*) - u_j\right]^2 w_j(\overrightarrow{x}^*) \tag{8}$$
The weighting function is often the standard SPH B3 spline.

- the SPH method applied to structural mechanics suffers from numerical instabilities. In [6], authors have shown that the Eulerian form of the SPH kernel w_{ij} exhibits a numerical instability in presence of tension stresses. The solution given in [7] consists in using a total Lagrangian formulation for which the kernel is stable.

- finally, most of the meshless methods suffers from the presence of zero energy modes due to the use of the collocation technique (strong form) or the nodal integration technique (weak form). This problem is extensively studied in [7]. Authors show that the use of a total Lagrangian formulation can reduce significantly the development of such zero energy modes. However, it is not sufficient in the case of a shell model because the field of the normals to the mean surface is very sensitive to instabilities that can occur in the curvature of the shell. [7] shows that the problem comes from the fact the kinematic variables and the strains and stresses are carried by the same nodes. The solution from [7] consists in introducing a second set a points denominated Stress Points (SP). These points a similar to Gauss points in the finite elements method (FEM) since they are only used to compute strains and stresses.

The SPH shell formulation is defined according to Mindlin-Reissner's thick shells theory. It relies on the assumption that the thickness e of the structure is small compared to its other dimensions, so the position vector $\overrightarrow{x}$ of any point located at a distance ξ from the mean plane can be expressed as:
$$\overrightarrow{x}(t) = \overrightarrow{x}_m(t) + \xi\overrightarrow{n}(t) \quad \xi \in \left[-\frac{e}{2}; +\frac{e}{2}\right] \tag{9}$$
$\overrightarrow{x}_m$ is the position of a point in the mean surface of the shell and $\overrightarrow{n}$ is the pseudo-normal vector that represents the orientation of the material. Mindlin-Reissner's shells theory takes

into account the influence of transverse shear on the model so that the pseudo-normal vector $\overrightarrow{n}$ does not remain normal to the mean plane. The displacement vector in the global coordinate system $R(x, y, z)$ is given as a function of the initial coordinates in the local coordinate system $R_{L0}(x_{L0}, y_{L0}, z_{L0})$ whose direction z_{L0} is normal to the shell:

$$\overrightarrow{u}\,(\overrightarrow{x}_{L0}, t) = \overrightarrow{u}_m(x_{L0}, y_{L0}, t) + z_{L0}\left[\overrightarrow{n}(x_{L0}, y_{L0}, t) - \overrightarrow{n}_0(x_{L0}, y_{L0})\right] \tag{10}$$

where $\overrightarrow{x}_{L0} = \mathbf{G}_{L0}\overrightarrow{x}_0$ and $\overrightarrow{n}_0$ is the initial pseudo-normal.

Green-Lagrange strain tensor in R_{L0} is given by:

$$(\mathbf{E})_{R_{L0}} = \frac{1}{2}\left[\frac{\partial\overrightarrow{u}_{L0}}{\partial\overrightarrow{x}_{L0}} + \frac{\partial\overrightarrow{u}_{L0}}{\partial\overrightarrow{x}_{L0}}^T + \frac{\partial\overrightarrow{u}_{L0}}{\partial\overrightarrow{x}_{L0}}^T\frac{\partial\overrightarrow{u}_{L0}}{\partial\overrightarrow{x}_{L0}}\right] = (\mathbf{E}^m)_{R_{L0}} + z_{L0}\left(\mathbf{E}^f\right)_{R_{L0}} \tag{11}$$

Tensor $\mathbf{E}^m$ contains membrane and transverse shear terms which are constant through thickness and $\mathbf{E}^f$ contains bending terms which vary linearly through thickness. Non-linear terms are taken into account.

Plane stresses assumption requires the application of the constitutive law in the mean plane of the shell in its current configuration. As a consequence, a local coordinate system $R_L(x_L, y_L, z_L)$ whose direction z_L is normal to the mean plane at the current point, is defined. Euler-Almansi strains corresponding to membrane and bending effects $(\overrightarrow{\varepsilon_{mf}})_{R_L}$ and transverse shear $(\overrightarrow{\varepsilon_c})_{R_L}$ are computed in R_L. Corresponding Cauchy stresses vectors $(\overrightarrow{\sigma_{mf}})_{R_L}$ and $(\overrightarrow{\sigma_c})_{R_L}$ are calculated through the use of a plane stresses constitutive law. Membrane and transverse shear resultants N_{ij} and T_i as well as bending moments m_{ij} are then obtained by integration of Cauchy stresses through thickness:

$$\begin{aligned} N_{ij} &= \int_{-e/2}^{e/2} \sigma_{ij}^m d\xi = e\sigma_{ij}^m \\ T_i &= \int_{-e/2}^{e/2} \sigma_{iz}^c d\xi = e\sigma_{iz}^c \\ m_{ij} &= \int_{-e/2}^{e/2} \xi\sigma_{ij}^f(\xi) d\xi = \frac{e^3}{12}\sigma_{ij}^f \end{aligned} \tag{12}$$

Because of the total Lagrangian formulation, the equilibrium equations are finally written in the global coordinate system R by means of Piola-Kirchoff 1 stresses.

3.2 Damage and fracture

Phenomena at the microscopic scale (microvoids and microcracks growth) leading to the failure of the shell are homogenized at the macroscopic scale through the use of continuum damage mechanics. A macroscopic crack appears in a reference volume element (RVE) once its damage variable reaches a critical damage value. The crack propagates at the structure scale when additional RVEs reach the critical damage value. Macroscopic cracks are treated as strong discontinuities in the SPH shell model.

3.2.1 Damage

For metals, damage comes from shear phenomena that favour the apparition of plasticity and from volumetric deformation that favours microvoids and microcracks growth. Damage criterion beyond which damage occurs is classical for this class of material and can be written [8]:

$$\left[\frac{2}{3}(1+\nu)+3(1-2\nu)\left(\frac{\sigma_H}{\sigma_{eq}}\right)^2\right]p-\epsilon_p^s \leq 0 \tag{13}$$

σ_H is the hydrostatic stress, σ_{eq} the equivalent Von-Mises stress, σ_H/σ_{eq} the triaxiality factor, ϵ_p^s an equivalent critical plastic strain, p the accumulated plastic strain and ν the Poisson's ratio. The damage evolution law is then given by [8]:

$$\dot{D}=\frac{D_c}{\epsilon_p^c-\epsilon_p^s}\left[\frac{2}{3}(1+\nu)+3(1-2\nu)\left(\frac{\sigma_H}{\sigma_{eq}}\right)^2\right]\dot{p} \tag{14}$$

ϵ_p^c is an equivalent critical plastic strain beyond which the material fails and D_c is the corresponding critical damage which is representative of the fraction of defaults (voids and cracks) in the RVE at failure. The damage evolution law must be coupled with a plasticity model (Von-Mises or Johnson-Cook plasticity for instance).

Numerical simulations performed with a material whose stress-strain curve presents a negative slope (softening or damaging material) are not satisfying since strains and damage are artificially localized in a single element when the failure is imminent. As a consequence, the energy dissipated in the fracture process and the failure time tend to zero as the mesh size decreases to zero. It means that microvoids and microcracks growth rate would be infinite, which is not physically acceptable. This problem is widely discussed in the literature [9] and is known as the numerical localization problem. Authors of [10] show that the problem comes from the transformation of the initial hyperbolic equations of the problems into elliptic equations when material softening occurs. As a consequence, the velocity of the waves in the material becomes complex which means they are trapped in the first element where softening occurs. Solutions proposed in the literature consists in preserving the initial hyperbolic form of the equation by introducing a characteristic length or time in model. This characteristic length or time is representative of the interaction of one element of the mesh with its neighbours. A characteristic time τ_c can be introduced in the model through the use of the following standard delayed damage model [11]:

$$\begin{aligned}&\text{if } D \leq D_c\\&\quad \dot{D}_r=\frac{1}{\tau_c}\left[1-e^{-a\langle D-D_r\rangle}\right]\\&\text{otherwise}\\&\quad \dot{D}_r=0\end{aligned} \tag{15}$$

D is the damage given by the damage evolution law, D_r is the regularized or delayed damage and $\langle . \rangle$ is the positive part operator. a is a second material parameter.

3.2.2 Damage-fracture transition

In the model presented in this paper, a crack is defined as the continuous set of fractured REV, see figure 2. This method is attractive since it does not require the explicit representation of the cracks, which simplifies the treatment of crack branching process for example.

Fully damaged REV are handled by introducing strong discontinuities into the model. As a consequence, interactions between SPH points (nodes or SP) through the cracked zone have to be deleted. Thus, the cracked zone is considered to be opaque such that points that are on

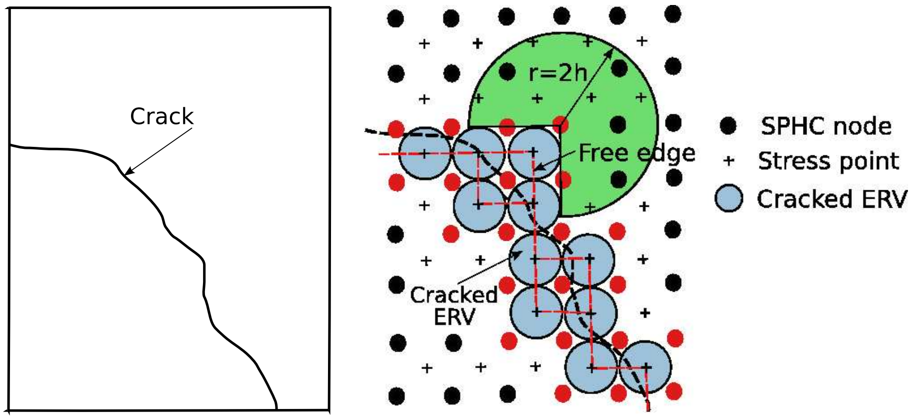

(a) Crack (b) SPHS Model

Figure 2: Modeling of a crack with SPHS model.

Remark: the method is illustrated with a regular quadrilateral mesh but it is applicable to any mesh constructed through a Vorono diagram.

the opposite side of the crack are excluded in the approximation of the displacement field. The shape of the support of the weighting functions is then represented in figure 2. This method is known as the visibility method [12]. In figure 2, it is obvious that some SPH points can come to the point where they do not have anymore neighbours. In this situation, if the point is a SP, it is chosen to eliminate it from the calculation by setting $D = D_c$. If the point is a node, it is kept in the calculation without interacting with the other points: its motion depends only on the kinetic energy he had at the time step he became a fragment and eventually on the contacts with other parts of the model. As a consequence, we keep two major advantages of meshless methods:

- fractures are simulated without mass and energy loss,
- fragments (i.e. SPH nodes without neighbourhood) can eventually interact with other parts of the model.

Finally, it is necessary to recompute MLS shape functions when fracture occurs since the neighbourhood of the nodes changes. The order of the polynomial basis used to compute MLS shape functions might be lowered when the number of neighbours decreases.

3.3 Numerical examples

3.3.1 Perforation of a plate

This test case is based on a work presented in [13] concerning the experimental and numerical analysis of the failure process of a mild steel sheet subjected to normal impact by hemispherical projectiles. A plug ejection was observed during experiments followed by a petalling process. The number of petals appearing during this process depends essentially on the velocity impact.

Figures 3(a) and 3(b) show the final state of the plate simulated with the SPHS method and compared with the calculations performed in [13] for an impact velocity $V_{imp} = 300 m.s^{-1}$. The model used in [13] is a FEM model with erosion of the element whose accumulated plastic strain exceeds a critical value. Failure time as a function of the impact velocity is ploted in figure 3(c) for SPHS model and calculations from [13]. The agreement between the various results is good.

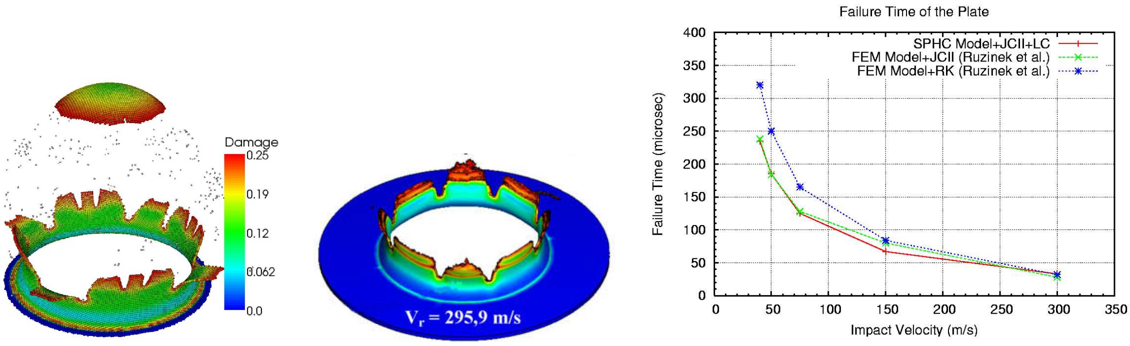

(a) SPHS Model (b) FEM Model [13] (c) Failure time

Figure 3: Perforation of a plate by an hemispherical projectile.

3.3.2 Fragmentation of explosively driven cylinders

This test case is based on an experimental work presented in [14] concerning the fragmentation of cylinders filled with a high explosive called LX-17. The cylinder is modeled with the SPHS method. The high explosive is modeled with FEM by using Jones-Wilkins-Lee equation of state which is characteristic of explosive materials. Figure 4(a) compares the fragments distribution obtained with the SPHS method with experimental data. Figure 4(b) represents the simulated fragments on the undeformed configuration of the cylinder.

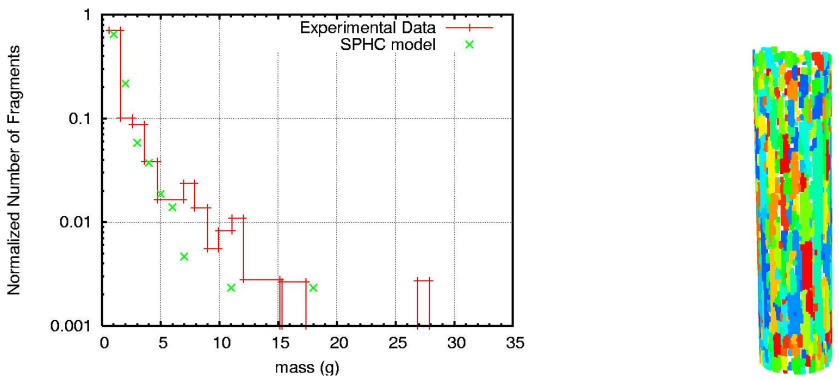

(a) Fragments distribution (b) Fragments identification

Figure 4: Fragmentation of explosively driven cylinders.

4 FLUID-STRUCTURE INTERACTIONS

Simulations of the failure of thin structures filled with fluid are complex problems for which the fluid-structure interface can change drastically during the transient. The Pinballs method [4] has already demonstrated its capability to handle this kind of problems in the FEM framework.

The method has been extended for the modeling of full SPH fluid-shell interactions in [15]. The main ingredients of the method are recalled in this section.

Each SPH node is filled with a so-called Pinball of spherical shape for fluid nodes and cylindrical shape for shell nodes. The detection of the contact then reduces to a simple geometrical interpenetration check between the Pinballs of the distinct contacting bodies. Once the contact is detected, contact forces are computed by enforcing impenetrability between the two impacting bodies. Contact forces should ensure that for a non viscous fluid:

$$(\overrightarrow{v_1} - \overrightarrow{v_2}).\overrightarrow{n} = 0 \tag{16}$$

where $\overrightarrow{v}_1$, $\overrightarrow{v}_2$ are the Pinballs velocities and $\overrightarrow{n}$ is a suitable normal direction to the contact surface. Much of the effectiveness and performance of the Pinballs algorithm depends on the choice made for the expression of $\overrightarrow{n}$. The method is primarily intended for impacts problems where sliding and friction are not crucial: the oscillations of the normal $\overrightarrow{n}$ to the interface (in the case of large radius Pinballs for example) can cause troubles in the case of two plane bodies sliding. In the particular case of the interaction between a SPH fluid and an SPH shell, the normal $\overrightarrow{n}$ is chosen to be the normal of the shell pinballs. The problem is solved through the use of Lagrange multipliers rather than penalty method which requires the introduction of a user-tuned parameter. This method is attractive since the contact detection requires simple geometrical checks. Moreover, the procedure is symmetric since both solids play the same role and no distinction is needed between a master and a slave.

5 APPLICATION: FAILURE PREDICTION OF A TANK UNDER IMPACT

The full SPH model presented in this paper is used to simulate the impact of a bullet onto a steel cylinder, according to the experimental conditions described in [16]. First, the cylinder is empty and the impact produces a simple perforation of the shell as can been seen in figure 5(a). The same was observed in the case of a cylinder filled with water for low velocity impacts. For high velocity impacts, for example $V_{imp} = 730m.s^{-1}$ in figure 5(c), the impact leads to a longitudinal crack and a fluid leakage.

Both the fluid and the cylinder are modeled with the SPH method described previously. The projectile is assumed to behave like a rigid body. In the case of an empty cylinder, the simulation predicts a simple perforation of the shell, see figure 5(b), which is in agreement with the experimental results. In the case of a water filled cylinder, the simulation predicts a longitudinal crack similar to the one observed in the experiment, see figure 5(d).

6 CONCLUSION

A full SPH method for the simulation of fluid-shell interactions until failure was presented in this paper. The fluid model is very classical in the SPH framework. The method has been extended to the simulation of fracturing shells by using the continuum damage mechanics and introducing strong discontinuities in the model once cracks appeared. The method is attractive since it does not require the explicit representation of the cracks, which simplifies the treatment of crack branching and fragmentation for example. Finally, the method is easily extended to fluid-structure interactions simulations through the Pinballs method. The model was developed in the fast dynamic software EUROPLEXUS.

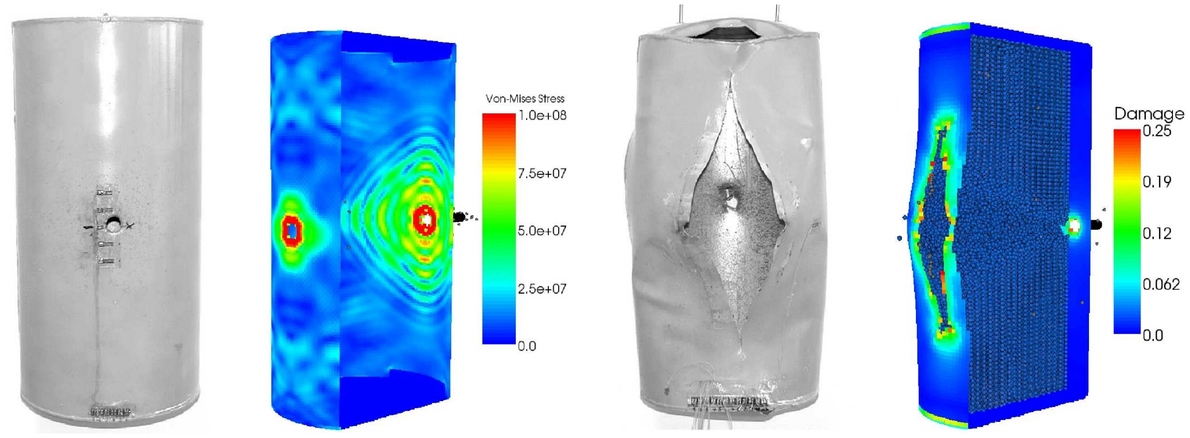

(a) Empty tank [16] (b) Empty tank SPH (c) Full tank [16] (d) Full tank SPH

Figure 5: Failure prediction of a tank under impact.

ACKNOWLEDGMENTS

The authors thank the French Atomic Energy Commission (CEA) and the French Electricity Company (EDF) for their support on the EUROPLEXUS software.

REFERENCES

[1] V.P. Nguyen, T. Rabczuk, S. Bordas, M. Duflot, Meshless methods: A review and computer implementation aspects. *Mathematics and Computers in Simulation*, **79**, 763-813, 2008.

[2] R.A. Gingold, J.J. Monaghan, Smoothed particle hydrodynamics: theory and application to non-spherical stars. *Monthly Notices of the Royal Astronomical Society*, **181**, 375-389, 1977.

[3] B. Maurel, A. Combescure, An SPH shell formulation for plasticity and fracture analysis in explicit dynamic. *International Journal for Numerical Methods in Engineering*, **76**, 949-971, 2008.

[4] T. Belytschko, MO. Neal, Contact-impact by the pinball method with penalty and Lagrangian methods. *International Journal for Numerical Methods in Engineering*, **31**, 547-572, 1991.

[5] G. A. Dilts, Moving least squares particle hydrodynamics - I : consistency and stability. *International Journal for Numerical Methods in Engineering*, **44**, 1115-1155, 1999.

[6] J.W. Swegle, D.L. Hicks, Y. Chen, Stabilizing SPH with conservative smoothing. SANDIA, *Report NSAN94-1932*, 1994.

[7] T. Belytschko, Y. Guo, W.K. Liu, S.P. Xiao, A unified stability analysis of meshless particle methods. *International Journal for Numerical Methods in Engineering*,**40**, 1359-1400, 2000.

[8] J. Lemaitre, J.-L Chaboche, *Mécanique des matériaux solides.* Dunod, 2004.

[9] Z.P. Bazant, Instability, ductility and size effect in strain softening concrete. *Mechanics and Journal of the Engineering Mechanics Division*, **102**, 331-344, 1976.

[10] Z.P. Bazant, T. Belytschko, Wave propagation in strain-softening bar: exact solution. *Journal of the Engineering Mechanics Division*, **111**, 381-389, 1985.

[11] O. Allix, J.-F. Deü, Delayed-damage modelling for fracture prediction of laminated composites under dynamic loading. *Engineering Transactions*, **45**, 29-46, 1997.

[12] T. Belytschko, L. Gu, Y.Y. Lu, Fracture and crack growth by element-free Galerkin methods. *Modelling and Simulation in Materials Science and Engineering*, **2**, 519-534, 1994.

[13] A. Ruzinek et al., Experimental and numerical study on the perforation process of mild steel sheets subjected to perpendicular impact by hemispherical projectiles. *International Journal of Impact Engineering*, **36**, 565-587, 2009.

[14] D.M. Goto et al, Investigation of the fracture and fragmentation of explosively driven rings and cylinders. *International Journal of Impact Engineering*, **35**, 1547-1556, 2008.

[15] B. Maurel, S. Potapov, S. Fabis, A. Combescure, Full SPH fluid-shell interaction for leakage simulation in explicit dynamics. *International Journal for Numerical Methods in Engineering*, **80**, 210-234, 2009.

[16] T. Timm, Beschuss von flssigkeitsgefllten Behltern. *PhD Thesis*, Karlsruhe University, Germany, 2003.